The Astrophysical Journal Letters, 723:L144–L148, 2010 November 10 doi:10.1088/2041-8205/723/2/L144

SUPERSONIC MAGNETIC UPFLOWS IN GRANULAR CELLS OBSERVED WITH SUNRISE/IMAX

J. M. Borrero[1,2], V. Martínez-Pillet[3], R. Schlichenmaier[1], S. K. Solanki[2,4], J. A. Bonet[3], J. C. del Toro Iniesta[5], W. Schmidt[1], P. Barthol[2], A. Gandorfer[2], V. Domingo[6], and M. Knölker[7]
[1] Kiepenheuer-Institut für Sonnenphysik, Schöneckstr. 6, D-79110 Freiburg, Germany; borrero@kis.uni-freiburg.de, schliche@kis.uni-freiburg.de, wolfgang@kis.uni-freiburg.de
[2] Max Planck Institut für Sonnensystemforschung, Max Planck Str. 2, Katlenburg-Lindau 37191, Germany; vmp@iac.es, solanki@mps.mpg.de, barthol@mps.mpg.de, gandorfer@mps.mpg.de
[3] Instituto de Astrofísica de Canarias, Avd. Vía Láctea s/n, La Laguna, Spain; jab@iac.es
[4] School of Space Research, Kyung Hee University, Yongin, Gyeongg 446-701, Republic of Korea
[5] Instituto de Astrofísica de Andalucía (CSIC), Apdo. de Correos 3004, 18080 Granada, Spain; jti@iaa.es
[6] Image Processing Laboratory, University of Valencia, P.O. Box 22085, E-46980 Paterna, Valencia, Spain; Vicente.Domingo-Codonyer@uv.es
[7] High Altitude Observatory (NCAR), 3080 Center Green Drive CG-1, Boulder, CO, USA; knoe@hao.ucar.edu
Received 2010 June 16; accepted 2010 August 12; published 2010 October 15

ABSTRACT

Using the IMaX instrument on board the Sunrise stratospheric balloon telescope, we have detected extremely shifted polarization signals around the Fe I 5250.217 Å spectral line within granules in the solar photosphere. We interpret the velocities associated with these events as corresponding to supersonic and magnetic upflows. In addition, they are also related to the appearance of opposite polarities and highly inclined magnetic fields. This suggests that they are produced by the reconnection of emerging magnetic loops through granular upflows. The events occupy an average area of 0.046 arcsec^2 and last for about 80 s, with larger events having longer lifetimes. These supersonic events occur at a rate of 1.3×10^{-5} occurrences per second per arcsec^2.

Key words: Sun: granulation – Sun: photosphere – Sun: surface magnetism

Online-only material: animations

1. INTRODUCTION

Unlike sunspots and active regions, the magnetic field in the solar granulation evolves at very short spatial and temporal scales as magnetic field lines are dragged and twisted by convective motions. This has made magnetic phenomenon in the quiet Sun particularly elusive and difficult to study. Recent instruments have achieved enough spatial resolution and temporal cadence to uncover some of these phenomena, such as emergence of magnetic loops: Centeno et al. (2007), Martínez González & Bellot Rubio (2009), Zhang et al. (2009), Martínez González et al. (2010); emergence of single polarity elements: Orozco Suárez et al. (2008); convective collapse in intergranular lanes: Bellot Rubio et al. (2001), Nagata et al. (2008), Fischer et al. (2009); horizontal supersonic velocities: Straus et al. (2010); supersonic downflows: Shimizu et al. (2007); shocks: Socas-Navarro & Manso Sainz (2005); vortex flows: Bonet et al. (2010); vortex tubes: Steiner et al. (2010); etc. In this Letter, we report on a phenomenon that has been uncovered by the IMaX instrument on board the Sunrise balloon. This phenomenon appears as highly shifted polarization signals within granular cells. They are usually associated with the presence of magnetic fields of opposing polarities in its vicinity. Highly inclined magnetic fields around these features are also commonly found, although not always connecting the two opposite polarities. Moreover, the long temporal series obtained with the IMaX instrument allow us to detect many events of similar characteristic and therefore to make statistics about their occurrence rate, lifetimes, and sizes.

2. INSTRUMENT AND DATA SET

Our data were recorded with the Imaging Magnetograph eXperiment (IMaX; Martínez Pillet et al. 2010) instrument on board the Sunrise balloon-borne observatory (Solanki et al. 2010; Barthol et al. 2010; Gandorfer et al. 2010). An average flight altitude of 35 km allowed Sunrise to avoid 99% of the disturbances introduced by Earth's atmosphere, which together with the Correlation-Tracker and Wavefront Sensor (CWS; Schmidt et al. 2004; Berkefeld et al. 2010) and the phase diversity calibration of the point-spread function of the optical system and further image reconstruction yielded spectropolarimetric data with a spatial resolution of 0.″15–0.″18 and a field of view (FOV) of 46″ × 46″ (after reconstruction).

Our IMaX data set comprises two observing sequences (of 22.7 and 31.6 minutes, respectively) recorded on June 9. Both sequences were taken close to the disk center in a quiet granulation region, although the second set contains a large network patch within the FOV. IMaX scans in four wavelength positions relative to $\lambda_0 = 5250.217$ Å: −80, −40, 40, 80 mÅ (hereafter denoted with the indexes λ_1,...,λ_4), across the magnetically sensitive ($g = 3$) Fe I 5250.217 Å spectral line. The HWHM (half-width at half-maximum) of IMAX's transmission profile is estimated to be 42.5 mÅ. This value includes the effect of the secondary peaks in the transmission profile. In addition, a fifth wavelength (continuum) point is measured: $\lambda_c = \lambda_0 + 227$ mÅ. At all five wavelengths, IMaX records the four polarization states of the light (Stokes I, Q, U, and V). Each full cycle (five wavelengths and four polarization states) is taken in about 32 s. The noise level is of the order of 3.5×10^{-3} in the reconstructed data. Each component of the Stokes vector is normalized to the average quiet-Sun continuum intensity: I_{qs} (also when not explicitly mentioned).

3. DETECTION AND DESCRIPTION

The data of Stokes $V(\lambda_c)$, or V_c, show a number of regions where the amount of circular polarization reaches values of (1.5–3) × 10^{-2}. Hereafter, we will refer to this features as supersonic magnetic events due to the large velocities in a

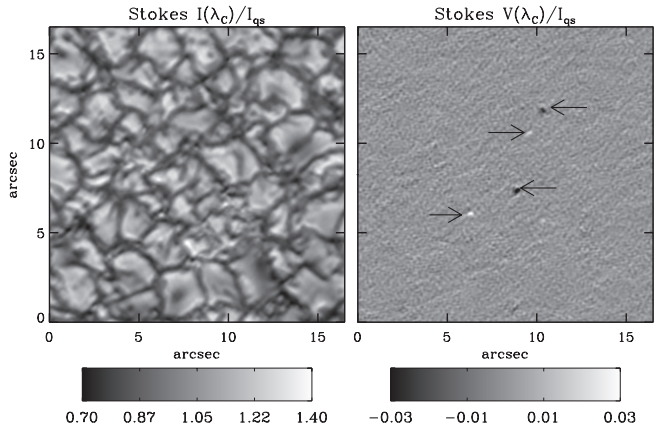

Figure 1. Left panel: reconstructed continuum intensity map (I_c) in a small region of IMaX's FOV. Right panel: circular polarization (V_c; +227 mÅ away from line center) map corresponding to the same region as the left panel. Indicated with arrows are four patches, where the circular polarization (absolute value) reaches values larger than 0.0125%.

magnetized plasma required to shift the polarization signal so far from the line center. Figure 1 (right panel) shows an extreme example where four of these features appear within a small ($15'' \times 15''$) FOV. Animations 1 and 2, available in the online edition of the journal, show these events. In our combined 54.3 minutes of observations, we have detected 4441 pixels belonging to 87 different events. This number of events yields a rate of occurrence of 1.3×10^{-5} events per second per arcsec^2. These events have been identified as the regions in each image that posses $|V_c| > 1.25 \times 10^{-2}$, and imposing that the patch must contain at least 9 pixels in order to match the instrument's spatial resolution.[8] Figures 2(a) and (b) display histograms of the size (in pixels) and lifetime of these events. Here, we also indicate with vertical dashed lines, the mean duration of these events (81.3 s), and their average size (15.5 pixels or 22720 km^2 at the disk center). Pearson's correlation coefficient between the lifetime and sizes of these events is 0.76, indicating that larger regions tend to live longer (Figure 2(c)).

Histograms in Figures 2(a) and (b) peak at the lower limit of our detection thresholds: 10 pixels in size and 32 s in lifetime. This suggests that there could be undetected events at smaller spatial scales and with shorter lifetimes. Although a minority, there are also some instances of events that embody areas larger than 25 pixels (10% of the total) or last more than 3 minutes (11.5% of the total).

Figure 3 displays I_c (upper row), V_c (middle row), and line-of-sight velocity v_{LOS} (bottom row), whereas Figure 4 displays the line-average circular polarization: $\frac{1}{4}\sum_{i=1}^{4}|V_i|$ (signed with the sign of V_1; upper row) and line-average linear polarization: $\frac{1}{4}\sum_{i=1}^{4}\sqrt{Q_i^2+U_i^2}$ (lower row) for three selected supersonic events. It is important to mention that the line-of-sight velocity in Figure 3 has been obtained from a Gaussian fit to the first four wavelength positions in Stokes I, therefore it should not be surprising that we do not see supersonic events here, but rather in V_c (second row) because this is where we have defined them. Also, the velocities presented here have already been corrected for the Sun's gravitational redshift, convective blueshift, and shifts caused by the collimated beam configuration of the instrument.

All three samples in Figures 3 and 4 occur at the center of granular cells: in regions with large blueshifted Doppler velocities and large continuum intensities. In fact, 72% of all detected events occur at the center or edges of granules, whereas only 8% appear in intergranular lanes. The remaining 20% occur in evolving granulation (i.e., on a granule that turns into an

[8] IMaX pixel size is 0.″055, therefore, 9 pixels occupy an area of 0.027 arcsec^2 which is comparable to the instrument's 0.15×0.18 arcsec^2 resolution.

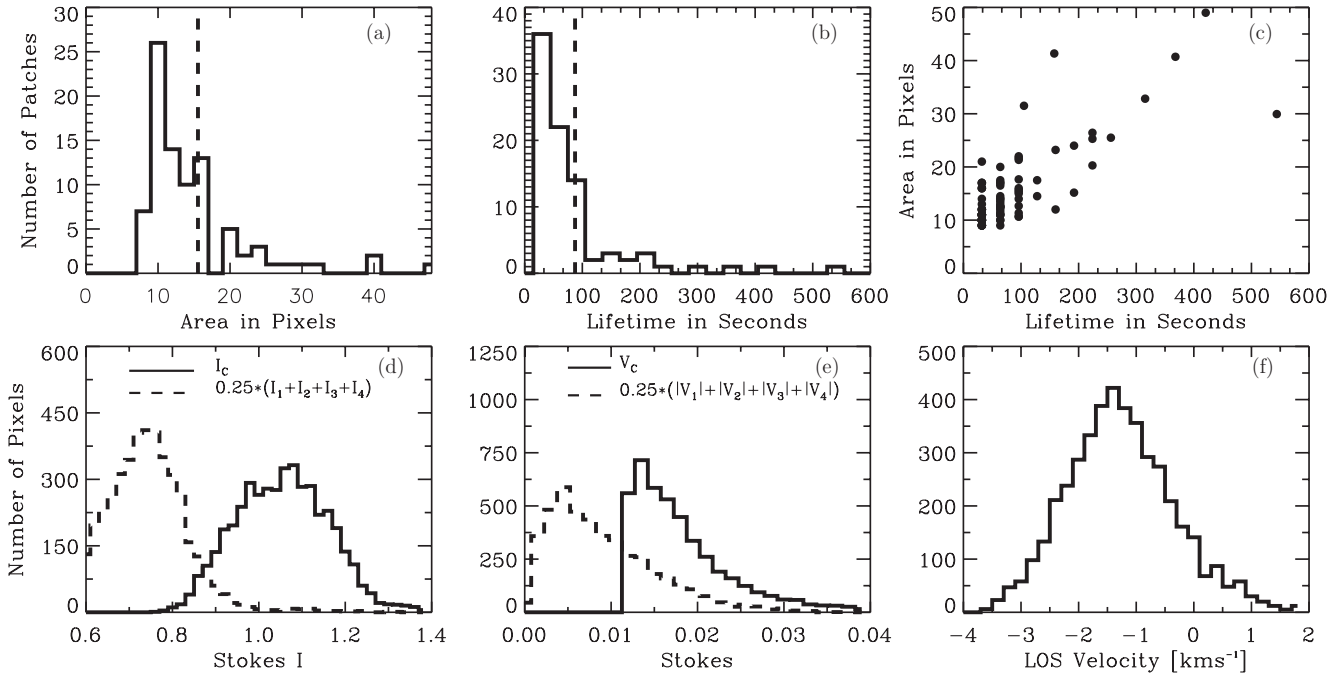

Figure 2. (a) Histograms of event area in number of pixels. (b) Histogram of events' lifetime. The vertical dashed line in the first two panels indicates the mean value of the size and lifetime, respectively. (c) Surface area as a function of lifetime for the 87 detected supersonic events. (d) Histogram of the number of pixels having a given line-average intensity (dashed) and a given continuum intensity I_c (solid). (e) Histogram of the number of pixels having a given line-average circular polarization (dashed) and a given continuum circular polarization V_c (solid). (f) Histogram for the line-of-sight velocity, obtained from the first four wavelengths in Stokes I, in the pixels displaying large values of V_c.

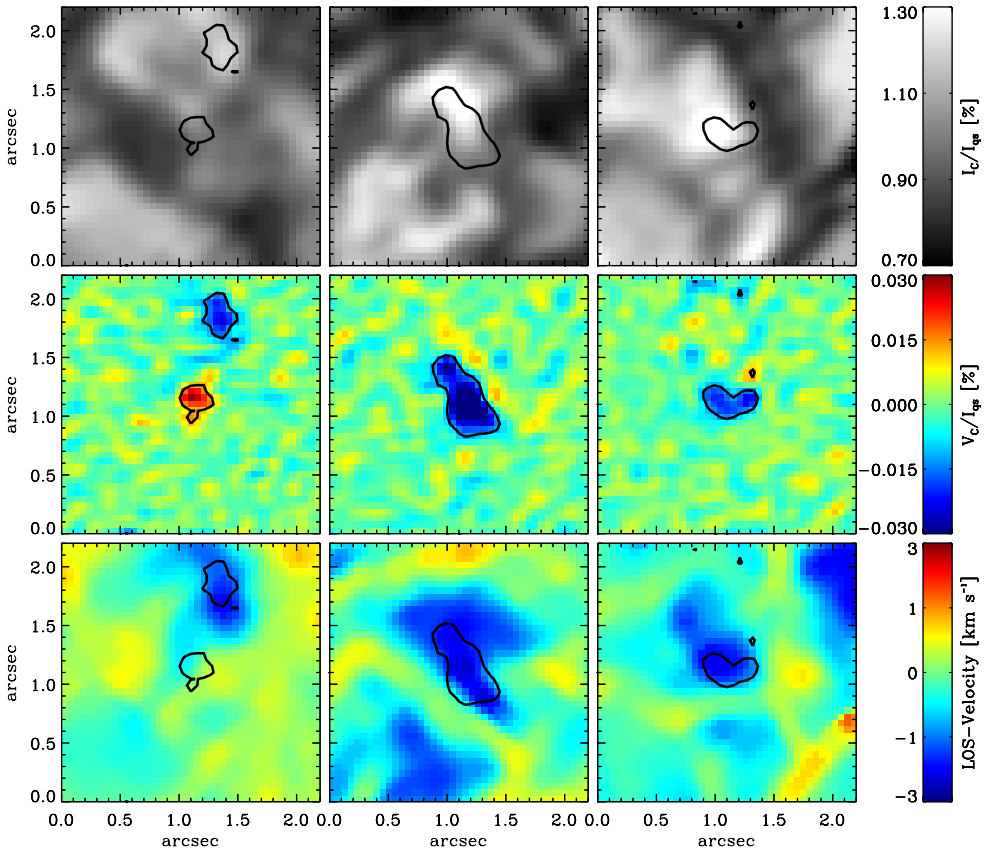

Figure 3. From top to bottom: continuum intensity I_c (normalized to the quiet-Sun average I_{qs}), continuum circular polarization V_c (normalized to the quiet-Sun continuum intensity I_{qs}), and line-of-sight velocity v_{LOS} (Gaussian fit to first four wavelengths of Stokes I). From left to right: three different examples of supersonic events found.

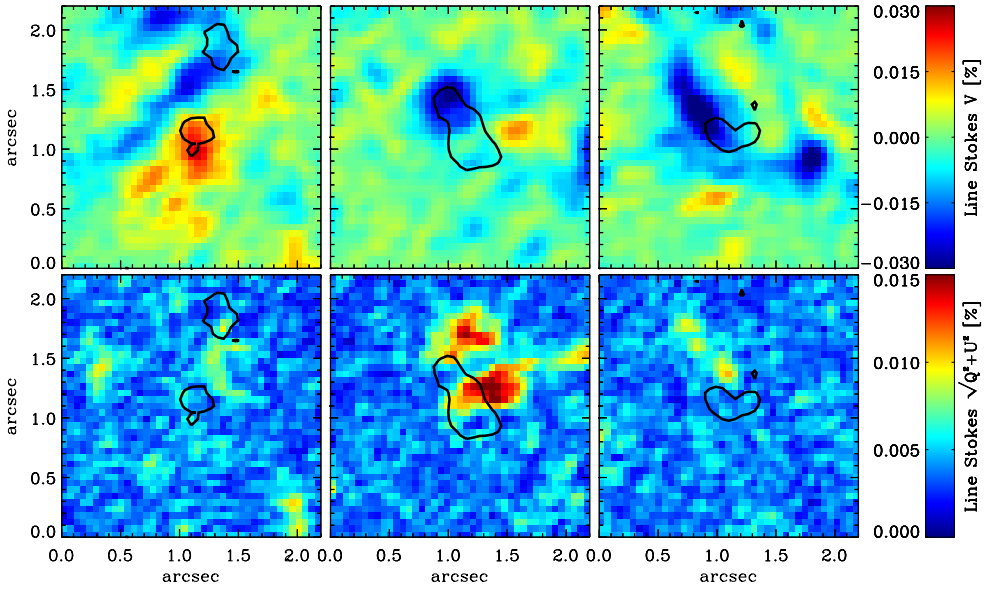

Figure 4. Same as Figure 3, but for the signed line-average circular polarization (top) and line-average linear polarization (bottom).

intergranule or vice versa) and might be related to exploring granules (Rast 1995).

In addition, the examples in Figures 3 and 4 show that sign of V_c bears no relation to the polarity of the magnetic field as V_c can have the same or opposite sign as V_l. In addition, most of the detected supersonic events appear as a single patch of large $|V_c|$, although sometimes (e.g., first event in Figures 3 and 4), specially in regions where the magnetic field topology is very complex, two supersonic patches appear together.

When looking at the vicinity of these events (FOV of 2″ around each), we observe that about 22% are associated with one single magnetic polarity in their neighborhood. In this case, the enhanced V_c occurs always at precisely the same location as this single polarity patch. The remaining 70% of all detected events are related to the appearance of opposite magnetic polarities

within 2″ of the supersonic events. Moreover, whenever opposite polarity regions are seen in the vicinity of the supersonic events, patches of enhanced linear polarization (not always connecting the opposing polarities) are observed (see also Danilovic et al. 2010). As seen in the line-averaged circular and line-averaged linear polarization (Figure 4) all three examples fall into this category. Although the levels of linear polarization (around 1%) are smaller than those of circular polarization (2%–3%), the fact that Stokes Q and U are clearly detected above the noise level is already evidence for the presence of highly inclined magnetic fields. The relation between the appearance of supersonic events and the existence of horizontal fields in their surroundings (in 70% of all cases) is showcased in Animations 3 and 4, available in the online journal.

Another feature of the supersonic events is that they do not stay always at the same position on the solar surface, but rather, they move horizontally with velocities typical of the granulation (1–2 km s^{-1}; cf. Straus et al. 2010).

The fact that most of the detected events are associated with the presence of magnetic fields of opposite polarity and inclined magnetic fields in their vicinity indicates that they are likely to be related to some form of magnetic reconnection. In addition (see Figure 2(f)), the supersonic events occur mostly in blueshifted regions, suggesting that the magnetic field emerges as it is dragged upward by upflowing granules. The same conclusion can be reached by looking at the solid line in Figure 2(d). This plot shows that the continuum intensity I_c is in most cases larger than 1.0, meaning that the supersonic events occur mainly in the brighter regions of the granulation (upflowing granules). A possible interpretation of these observations is that the supersonic magnetic flows are associated with the emergence of magnetic loops (where the field is horizontal) that reconnect with the pre-existing ambient magnetic field. The footpoints on this loop would be seen as the opposite polarities that we observe in many of the cases.

4. DISCUSSION AND CONCLUSIONS

Since the line-of-sight velocities associated with these events are mostly blueshifted, we surmise that the signal we observe in V_c (+227 mÅ on the red side of $\lambda_0 = 5250.217$ Å; see Figure 1) is not due to a redshifted contribution from Fe I 5250.217 Å, but rather a blueshifted contribution from the nearby line Fe I 5250.653 Å.[9] Note that the continuum wavelength λ_c is almost as far from Fe I 5250.217 as from Fe I 5250.653.

In principle, a wavelength difference of 227 mÅ corresponds to a Doppler shift of 12 km s^{-1}. However, a better estimation that considers the widths of the spectral line and IMAX's transmission profile, yields a possible range of $v_{LOS} \in [5, 12]$. Because of projection effects, v_{LOS} represents only a lower limit of the absolute velocity. Taking into account that the speed of sound in the solar photosphere is about $c_s \simeq 6$ km s^{-1}, this points toward potentially supersonic line-of-sight velocities. With the current data, however, we do not sample the spectral region well enough to narrow down further the range of possible velocities.

One problem facing an interpretation in terms of supersonic upflows is that, if Fe I 5250.653 Å was affected by 12 km s^{-1}upward velocities, we would observe (along with large V_c signal) a decrease in the I_c signal, since the absorption line would have also shifted from 5250.653 Å into λ_c. However, Figure 2(d) indicates that the intensity observed at λ_c (solid line) is much larger than the mean intensity observed around the spectral line Fe I 5250.217 Å (dashed line), suggesting that not the whole line is shifted. On the other hand, smaller velocities ($v_{LOS} \approx -4$ km s^{-1}) do not help solve the puzzle either, since then the line-average circular polarization in Fe I 5250.217 Å would still be rather large, in particular, much larger than the circular polarization in the continuum V_c. However, as shown in Figure 2(e), V_c (solid line) is larger than the line-average circular polarization (dashed line).

We have not studied in detail additional complications such as strong gradients along the line-of-sight or the presence of unresolved structures within the area occupied by the supersonic event, which produce peculiar Stokes profiles and ought to be analyzed in a different way. Note however, that in both of these cases, extremely large velocities at some height in the atmosphere or within a small portion of the resolution element, must still be invoked (see, for example, Figure 4 in Socas-Navarro & Manso Sainz 2005). An additional effect that we have not considered here, but which may be important to explain the seemingly contradictory behavior described in the previous paragraph, is the fact that, if indeed these events are related to magnetic reconnection (as supported by the presence of opposite magnetic polarities), one or both spectral lines, could appear in emission, making it possible to have large blueshifted velocities without noting a decrease in I_c, but rather an increase.

The German contribution to SUNRISE is funded by the Bundesministerium für Wirtschaft und Technologie through Deutsches Zentrum für Luft-und Raumfahrt e.V. (DLR), Grant No. 50 OU 0401, and by the Innovationsfond of the President of the Max Planck Society (MPG). The Spanish contribution has been funded by the Spanish MICINN under projects ESP2006-13030-C06 and AYA2009-14105-C06 (including European FEDER funds). The HAO contribution was partly funded through NASA grant NNX08AH38G. This work has been partly funded by the WCU grant R31-10016 funded by the Korean Ministry of Education, Science and Technology.

REFERENCES

Barthol, P., et al. 2010, Sol. Phys., in press (arXiv:1009.2689)
Bellot Rubio, L. R., Rodríguez Hidalgo, I., Collados, M., Khomenko, E., & Ruiz Cobo, B. 2001, ApJ, 560, 1010
Berkefeld, T., et al. 2010, Sol. Phys., in press (arXiv:1009.3196)
Bonet, J. A., et al. 2010, ApJ, 723, L139
Centeno, R., et al. 2007, ApJ, 666, L137
Danilovic, S., et al. 2010, ApJ, 723, L149
Fischer, C. E., de Wijn, A. G., Centeno, R., Lites, B. W., & Keller, C. U. 2009, A&A, 504, 583
Gandorfer, A., et al. 2010, Sol. Phys., in press (arXiv:1009.1037)
Martínez González, M., & Bellot Rubio, L. R. 2009, ApJ, 700, 1391
Martínez González, M., Manso Sainz, R., Asensio Ramos, A., & Bellot Rubio, L. R. 2010, ApJ, 714, L97
Martínez Pillet, V., et al. 2010, Sol. Phys., in press (arXiv:1009.1095)
Nagata, S., et al. 2008, ApJ, 677, L145
Orozco Suárez, D., Bellot Rubio, L. R., de Toro Iniesta, J. C., & Tsuneta, S. 2008, A&A, 481, L33
Piskunov, N. E., Kupka, F., Ryabchikova, T. A., Weiss, W. W., & Jeffery, C. S. 1995, A&AS, 112, 525

[9] We have conducted a spectral line search in the NIST (http://physics.nist.gov/PhysRefData/ASD/lines_form.html) and the VALD databases (Piskunov et al. 1995) and found only this other spectral line in the vicinity of Fe I 5250.217 Å.

Rast, M. 1995, ApJ, 443, 863
Schmidt, W., et al. 2004, Proc. SPIE, 5489, 1164
Shimizu, T., Martinez-Pillet, V., Collados, M., Ruiz-Cobo, B., Centeno, R., Beck, C., & Katsukawa, Y. 2007, in ASP Conf. Ser. 369, New Solar Physics with Solar-B Mission, ed. K. Shibata, S. Nagata, & T. Sakurai (San Francisco, CA: ASP), 113
Socas-Navarro, H., & Manso Sainz, R. 2005, ApJ, 620, L71
Solanki, S. K., et al. 2010, ApJ, 723, L127
Steiner, O., et al. 2010, ApJ, 723, L180
Straus, T., Fleck, B., Jefferies, S. M., Carlsson, M., & Tarbell, T. D. 2010, in Proc. 25th NSO Workshop, Chromospheric Structure and Dynamics: From Old Wisdom to New Insights, ed. A. Tritschler, K. Reandon, & H. Uitenbroek, in press (arXiv:1002.3305)
Zhang, J., Yang, S.-H., & Jin, C.-L. 2009, Res. Astron. Astrophys., 9, 921